Hindawi Publishing Corporation
Advances in Optical Technologies
Volume 2008, Article ID 275080, 7 pages
doi:10.1155/2008/275080

Research Article

A Proposed Method for Thermal Specific Bioimaging and Therapy Technique for Diagnosis and Treatment of Malignant Tumors by Using Magnetic Nanoparticles

Iddo M. Gescheit, Moshe Ben-David, and Israel Gannot

Department of Biomedical Engineering, Faculty of Engineering, Tel-Aviv University, Tel-Aviv 69978, Israel

Correspondence should be addressed to Israel Gannot, iddog@medingo.com

Received 25 February 2008; Accepted 9 April 2008

Recommended by Stoyan Tanev

The objective of this research program is to develop a novel, noninvasive, low-cost infrared (8–12 μm spectral range) imaging technique that would improve upon current methods using nanostructured core/shell magnetic/noble metal-based imaging and therapies. The biocompatible magnetic nanoparticles are able to produce heat under AC magnetic field. This thermal radiation propagates along the tissue by thermal conduction reaching the medium's (tissue's) surface. The surface temperature distribution is acquired by a thermal camera and can be analyzed to retrieve and reconstruct nanoparticles' temperature and location within the tissue. The technique may function as a diagnostic tool thanks to the ability of specific bioconjugation of these nanoparticles to tumor's outer surface markers. Hence, by applying a magnetic field, we could cause a selective elevation of temperature of the targeted nanoparticles up to 5°C, which detects the tumor. Furthermore, elevating the temperature over 65°C and up to 100°C stimulates a thermo ablating interaction which causes a localized irreversible damage to the cancerous site with no harm to the surrounding tissue. While functioning as a diagnostic tool, this procedure may serve as a targeted therapeutic tool under thermal feedback control as well.

1. INTRODUCTION

Cancer is a very prevalent disease with no satisfying cure and/or treatment. American Cancer Society statistics shows that about 1 399 790 new cancer cases were diagnosed in 2006. This number does not include carcinoma in situ (noninvasive cancer) or any site except urinary bladder, and does not include basal and squamous cell skin cancer. More than 1 million cases of basal and squamous cell skin cancers were diagnosed in 2006. In the same year, about 564 830 Americans died of cancer, more than 1 500 people a day. Cancer is the second most common cause of death in the US, exceeded only by heart disease. In the US, cancer accounts for 1 out of every 4 deaths. The National Institute of Health (NIH) estimates overall costs for cancer in 2005 with $209.9 billion [1–3].

Conventional (anatomical, structural) imaging is insensitive to the presence of cancer, often failing to yield the very information needed for accurate diagnosis and staging, for proper treatment selection and monitoring or for effective followup after treatment. For example, small primary tumors go undetected. For many cancers, an internal, aggressive, noncalcified tumor under containing fewer than 500 000 cells (i.e., under 2 mm wide) is likely to pass undetected through most body-region scans, including CT, MRI, ultrasound, radionuclide, and metabolic PET. At this size, a tumor has effectively undergone 19 cell doublings about halfway through doubling toward a predicted lethal load of $10^{10}-10^{12}$ cells and is likely to be sufficiently repleted with gene defects so that it will undergo continued and uninterrupted growth if not treated [4].

While cancer may be suspected for a variety of reasons, the definitive diagnosis of most malignancies must be confirmed by histological examination of the cancerous cells by a pathologist. After obtaining tissue sample by a biopsy or surgery, the tissue diagnosis indicates the type of cell that is proliferating, its histological grade and other features of the tumor. Together, this information is useful

to evaluate the prognosis of this patient and choose the best treatment. However, current therapy techniques (e.g., surgery, chemotherapy, radiation) still show poor results and therefore, unfortunately, the standard of care is to blindly treat with chemotherapy selected by convention using prior retrospective studies. A treatment is considered a success or failure only in retrospect (i.e., success is when a patient survives 5 years, and failure is when a relapse occurs).

Hence, the majority of diagnosis and therapy modalities is not capable of distinguishing between malignant cells and healthy tissue (especially in early stages) and does not provide the physician with adequate precision and specificity. Moreover, there is no real-time control referring to the physiological margins distinguishing the malignant and benign tissue. The implications of the latter are, for example, in surgery: if the surgeon does not remove all the malignant cells, the progression or recurrence of the disease is almost without doubt. On the other hand, if the surgeon removes more than necessary, the "extra" tissue being removed is a healthy tissue and may be vital for the organ-life cycle or patient's life.

2. MATERIALS AND METHODS

2.1. The system

The suggested system and method are schematically depicted in Figure 1. After the insertion of magnetic nanoparticles into a patient's body (either locally to a suspected tissue or systematically to the blood stream by IV injection), the nanoparticles arrive in short proximity to the tumor and a process of bioconjugation occurs in compliance with a pharmacokinetic profile. Thus, the tumor's outer surface is bound with nanoparticles by virtue of strong chemical bonds configured as antigen-antibody complex. Since the biocompatible magnetic nanoparticles are able to produce heat under AC magnetic field, the region of interest (ROI) is placed under a suitable field. This emitted thermal radiation propagates along the tissue by thermal conduction reaching medium's (tissue's) surface. The surface temperature distribution is acquired by a thermal camera and could be analyzed to retrieve and reconstruct nanoparticles' temperature and location within the tissue. In future minimal invasive applications, the IR radiation can be "guided" from internal compartments of the body to the outside by waveguides and dedicated optical fibers, for example, thermal imaging bundles shown by Gannot et al. [5–8].

By elevating the temperature of the conjugated nanoparticles up to ~5°C, diagnosis is enabled while elevation of local temperature over 65°C allows "clean treatment," that is, localized irreversible damage to the cancerous site almost without harming the surrounding tissue.

2.2. Bioconjugation

A fundamental issue lying on the basis of this system is the fact that the magnetic nanoparticles are localized specifically and functions as mediators situated on the periphery of the tumor. In order to target the tumor

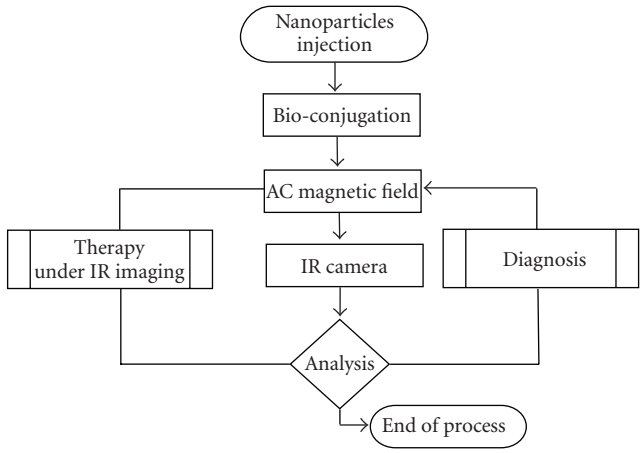

Figure 1: Schematic description of the system employing a targeted imaging technique and a closed-loop system for therapy under real-time feedback.

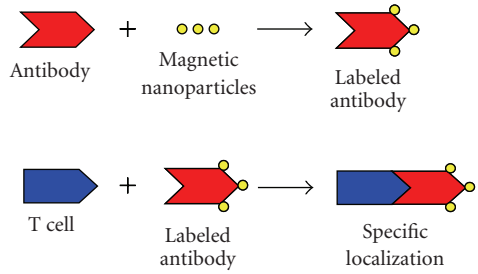

Figure 2: Bioconjugation of magnetic nanopatricles by using the natural immune system.

and deliver the nanoparticles reliably and specifically, the suggested transportation leans on human's immune system. The malignant tumor tends to present specific antigens on its outer surface. These antigens are able to communicate with corresponding agents of the immune system (e.g., antibodies) to establish antigen-antibody complexes which are characterized in strong chemical bonds. For instance, we can bind the magnetic nanoparticles' surface to the antibodies via adhering polymers (e.g., PEG) so that antibodies transfer them towards the tumor being delivered by immune agents (T-cell), and conjugate them to the tumor, retaining them along the tumor's outer surface (Figures 2 and 3).

This bioconjugation is analogous to that made with fluorophores in research conducted by Fibich et al. [9] and Gannot et al. [10].

2.3. Heat generation

There exist at least three different mechanisms by which magnetic materials can generate heat in an alternating field [11]:

(i) generation of eddy currents in bulk magnetic materials;

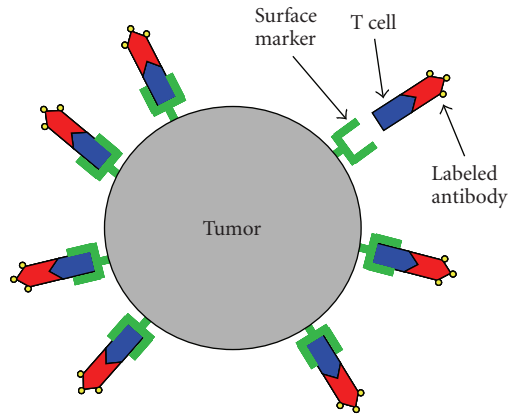

Figure 3: Magnetic nanoparticles schematic siting along the tumor surface.

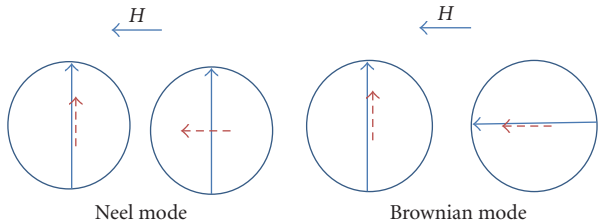

Figure 4: Relaxational losses leading to heating in an alternating magnetic field (H).

(ii) hysteresis losses in bulk and multidomain magnetic materials

(iii) relaxation losses in "superparamagnetic" single-domain magnetic materials.

In this technique, we use single-domain particles in which mechanism (i) and (ii) contribute very little to the heating of these particles (if at all) [12], while the significant mechanism in contribution with heating is the relaxation mechanism (iii) [13, 14].

Relaxation losses in single-domain magnetic nanoparticles fall into two modes: (a) rotational (Brownian) mode and (b) Néel mode [13, 15]. The principle of heat generation due to each individual mode is shown in Figure 4.

In the Néel mode (Figure 4(a)), the magnetic moment (dotted arrow) originally locked along the crystal easy axis (solid arrow) rotates away from the crystal axis towards the external field (H). The Néel mechanism is analogous to the hysteresis loss in multidomain magnetic particles whereby there is an "internal friction" due to the movement of the magnetic moment in an external field that results in heat generation.

In the Brownian mode (Figure 4(b)), the whole particle oscillates towards the field with the moment locked along the crystal axis under the effect of a thermal force against a viscous drag in a suspending medium. This mechanism essentially represents the mechanical friction component in a given suspending medium [16].

Each of the relaxation modes that lead to heat generation is characterized by a time constant. τ_N is the Néel time constant given by

$$\tau_N = \tau_0 \exp\left(\frac{E_B}{k_B T}\right), \tag{1}$$

where $E_B = K_u V$ is analogous to an activation energy that has to be overcomed by the thermal energy $k_B T$ to overcome the inherent magnetic anisotropy energy.

The energy barrier E_B is represented by the constant K_u, which is a material property and is the anisotropy constant, multiplied by V, which is the volume of the magnetic nanoparticle. The thermal energy is represented by the constant k_B, named by Stephan Boltzmann, and multiplied by the absolute temperature T. The constant τ_0 is of the order of 10^{-9} seconds [13].

The Brownian time constant represented by τ_B is given by

$$\tau_B = \frac{3\eta V_H}{k_B T}, \tag{2}$$

where V_H is the hydrodynamic volume of the magnetic nanoparticle which is the effective volume (including that of the nanoparticle and coating or surfactant attached to the nanoparticle), η is the viscosity of the liquid carrier, and $k_B T$ is the thermal energy.

The resultant power generation is a strong function of the effective time constant, and the field parameters and is given by

$$P_{SPM} = \pi \mu_0 \chi_0 H_0^2 f \frac{2\pi f \tau}{1 + (2\pi f \tau)^2}, \tag{3}$$

where H_0 and f are the amplitude and frequency of the applied alternating magnetic field, respectively, χ_0 is the magnetic susceptibility, μ_0 is the permeability of free space, and τ is the effective time constant given by $1/\tau = (1/\tau_N) + (1/\tau_B)$ [11, 13].

2.4. Affecting parameters

There are numerous parameters affecting the heat generation, which is produced by magnetic nanoparticles excited by a magnetic field. A few examples for some crucial parameters are given below which one should take into consideration when heating with magnetic nanoparticles.

2.4.1. Field parameters

According to (3), it is obvious that field strength and frequency are controllable parameters that directly affect the power produced by the nanoparticles when alternative magnetic field is applied. It should be understood that the of field parameter is not simply proportional to the generated power but more complex, and depends on additional parameters such as the nanoparticles' material properties [17].

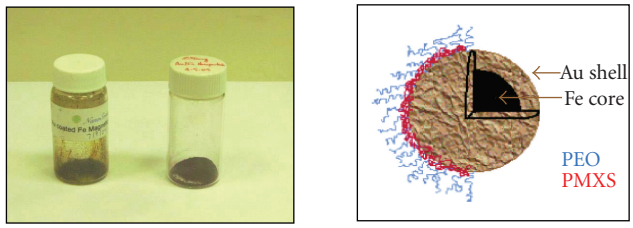

(a) (b)

Figure 5: Fe Nanoparticles produced by Nanosonics Inc. (a) Magnetic nanoparticles in different particle size configured as powder. (b) Schematic illustration of a single Fe-Au nanoparticle.

2.4.2. Material properties

An interesting class of magnetic materials that are common for this purpose is iron oxides such as Fe_3O_4, γ-Fe_2O_3 and $MO{\cdot}Fe_2O_3$ (where M is Mn, Co, Ni, Cu) [18], because they display ferrimagnetism. Magnetite (Fe_3O_4), meghemite (γ-Fe_2O_3), and hematite (α-Fe_2O_3) are the most common iron oxides and they are discussed below.

Another alternative is the magnetic nanoshells which were designed and characterized by Nanosonic Inc. (Figure 5(a)). The nanoshells are comprised of an iron core with diameter of 8 nm coated with a layer of gold. The gold coatings are made in order to prevent oxidation, hence demagnetization; ultrathin noble metal coatings of Au (~2 nm) were prepared to provide long-term stability and biocompatibility for the Fe core. The Fe core was coated with a series of block copolymer stabilizers that are compatible with analgesics to prevent flocculation in the arterial system in vivo (see Figure 5(b)). In addition, the block copolymers assist in preventing agglomeration.

Other materials are also being investigated including platinium compounds, vanadium oxides, cobalt, nikel, lanthanum, and manganase [19, 20].

2.4.3. Size dependence

The size of the nanoparticles is a fundamental characteristic in this field. Ma et al. [21] investigated the specific absorption rate (SAR) values of aqueous suspensions of magnetite particles with different diameters varying from 7.5 to 416 nm by measuring the time-independent temperature curves in an external altering magnetic field

(80 kHz, 32.5 kA/m). Results indicate that the SAR values of magnetite particles are strongly size dependent. For magnetite larger than 46 nm, the SAR values increase as the particle size decreases where hysteresis loss is the main contribution mechanism. For magnetite particles of 7.5 and 13 nm which are superparamagnetic, hysteresis loss decreases to zero and, instead relaxation losses (Néel loss and Brownian rotation loss) dominate.

The dividing line between the two cases depicted above is given by the ferromagnetic exchange length $d_{ex} \cong \sqrt{A/K}$ using the material parameters of magnetite ($K = 1.35 \times 10^4$ J/m^3, $A = 10^{-11}$ J/m), the exchange length is estimated as $d_{ex} \cong 27$ nm.

Therefore, when the particle size is larger than d_{ex}, the hysteresis loss increases as the particle size decreases. However, once the particle size is less than d_{ex}, hysteresis loss will vanish and the main contribution will be of relaxation losses, as shown, for example, by Ma et al. [21]. In addition, Hergt et al. show that in the critical particles size region where hysteresis losses vanish, Néel losses grow as a new loss mechanism which, roughly speaking, extends the loss region toward even smaller particle sizes [12].

2.4.4. Other parameters

The parameters discussed above are merely a few examples for a larger collection of affecting parameters. Some of them have been investigated and some are probably yet unknown. Amongst them is the concentration of the nanoparticle inserted into the body [11]. The concentration should be large enough to effectively produce heat, but yet in an amount that will not be toxic for the human body. One also needs to be aware of the evacuation of those particles once their job is done. (We are not dealing with toxicity and pharmacokinetics issues in this paper.) The coating of nanoparticles (e.g., derivatives of dextran, polyethylene glycol (PEG), polyethylene oxide (PEO), and poloxamers and polyoxamines) and suspending medium also affect the heat generation [11, 16, 22]. The period of time of excitation filed application and profile (e.g., continuous, pulsatile) deeply affects the SAR which is proportional to the power dissipated [23]. Another affecting parameter under investigation is the presence of nanoparticles' agglomeration in comparison with the heat generated in single or dispersed nanoparticles [24].

2.5. Thermal analysis

Upon the heating of the bioconjugated nanoparticles, we generate a heat source within the body. The heat source, namely the tumor, and in particular the tumor's surface, is actively heated by external and controlled magnetic fields. Based on a two dimensional thermal image acquired from the tissue surface, we seek to derive two fundamental characteristics: the *depth* of the tumor and the *temperature* of the tumor and its surroundings. Knowing the temperature in real-time is crucial in order to avoid any damage to all tissues in the diagnostic mode on one hand, and on the other hand, operating in therapeutic mode, we expect to damage only the malignant tissue leaving the healthy surrounding tissue with minimal damage. There are various techniques for analyzing the thermal data such as, for example, automatic segmentation approaches, and feature extraction and classification as shown by Qi and Diakides [25].

2.6. Setup

The main building blocks of the suggested system are comprised of means for (shown in Figure 6):

(i) heat generation;

(ii) thermal image acquisition;

(iii) thermal image analysis;

(iv) heat generation.

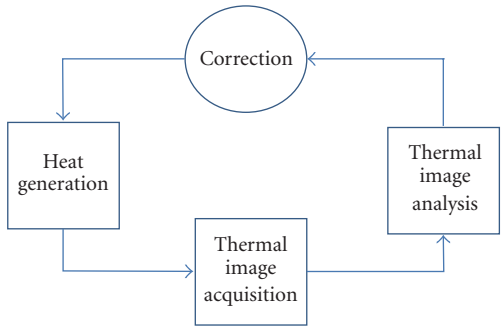

Figure 6: Schematic description of the system.

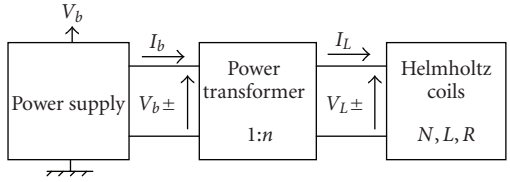

Figure 7: System's block scheme.

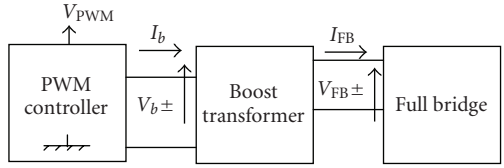

Figure 8: The power generator's block scheme.

Heat generation is conceptually comprised of two parts:

(i) magnetic nanoparticles (for "heat emission");

(ii) magnetic field (for nanoparticles' excitation).

The magnetic field is generated by a magnetic system usually comprised of the following:

(i) antenna (e.g., coils)

(ii) AC current generator.

The design of the magnetic system is implemented bottom-to-up, that is, after choosing the desirable field parameters (e.g., field strength, frequency), we are capable of designing the system itself (e.g., coils, circuitry). Determination of the desirable parameters is not trivial since the system is characterized by a large number of degrees-of-freedom.

Previous research works investigated various fields: Kalambur et al. used a 1 kW generator and 4 turn RF coils to produce field strength of $H_0 = 14$ [kA/m] and frequency $f = 175$ [kHz]; Giri et al. examined the fields (10–45[kA/m], 300 [kHz]);

Ma et al. used a 15 kW RF generator to produce the field (32.5 [kA/m], 80 [kHz]); Hergt et al. (2004) showed losses under the AC field (11 [kA/m], 410 [kHz]); Pankhurst et al. investigated nanoparticles under the extensive field region of (0–15 [kA/m], 0.0.5–1.2 [MHz]) and Kim et al. examined the influence of fields of (110 [kA/m], 0.1–15 [MHz]).

The two principle parameters of the externally applied magnetic field, that is, the frequency and strength, are limited by deleterious physiological responses to high-frequency magnetic fields [26, 27]: stimulation of peripheral and skeletal muscles, possible cardiac stimulation and arrhythmia, and nonspecific inductive heating of tissue. Generally, the useable range of frequencies and amplitudes is considered to be $f = 0.05$–1.2 MHz and $H = 0$–15 kA/m.

Experimental data on exposure to much higher frequency fields come from groups such as Oleson et al. [28] who developed a hyperthermia system based on inductive of tissue, and Atkinson et al. who developed a treatment system based on eddy current heating of implantable metal thermoseeds. Atkinson et al. [29] concluded that exposure to fields where the product $H \cdot f$ does not exceed 4.85×10^8, kA/(m·s)$^{-1}$ is safe and tolerable [30].

Hence, following the physiological constraints shown above and based on previous research results such as those mentioned above, the desirable averaged working point was chosen to be $H_0 \approx 10$ [kA/m]; $f \approx 100$ [kHz].

Trying to meet with the fundamental objectives of the suggested system, particularly cost effectiveness and bedside capability, we seek an alternative technology for the commonly used giant and expensive RF generators of several kilowatts and up, since they cost about 10 k–100 k of dollars and are not comfortable to be located near the patient's bed or at the clinic. Most of research works in this field are using a single RF coil with a few turns, for example, 3-4 turns. A major drawback of the coil configuration is that there is no accessibility for any imaging element, such as an IR camera. If we had desired to use that kind of solenoid coil, it would have been characterized with a very large diameter, and the camera would have been exposed to the AC field. Hence, this configuration is not applicable and does not apply to our needs.

An alternative preferred method relies on a Helmholtz coil configuration. The fundamental premise of this configuration is that it produces a uniform (homogeneous) magnetic field between the coils with the primary field component parallel to the axes of the two coils. The Helmholtz configuration further enables an open workspace for sample (tissue) handling and imaging device accessibility, that is, an easy and safe path for placing the IR camera, and further enables the change of the distance between the two coils, that is, adjustable workspace.

In order to produce a desired high voltage over the coils, the system design includes power transformer for voltage elevation, as shown in Figure 7.

The power supply of the system is composed of an oscillator (PMW controller) with a tunable frequency, boost transformer, and a push-pull full bridge inverter (H-bridge), as shown in Figure 8. The full bridge is mainly composed of four FETs to allow the alternate current.

The thermal imaging is carried out by an IR camera (FLIR A40M), which detect the infrared emission which is

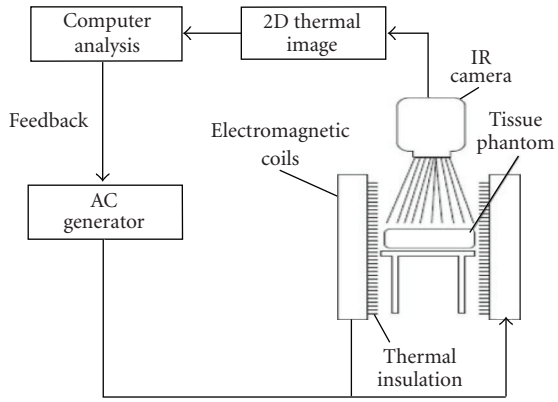

Figure 9: Schematic description of the closed-loop system.

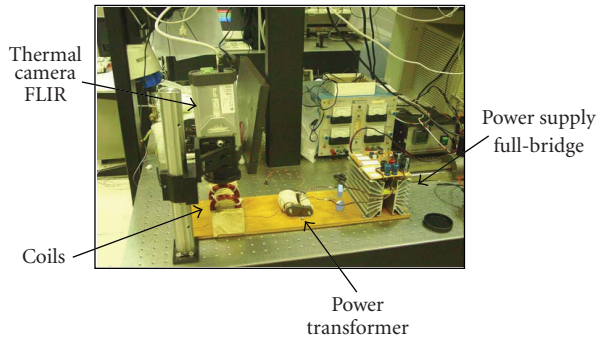

Figure 10: Laboratory system.

emitted from the examined object's surface (e.g., phantom).

The IR camera is positioned perpendicularly above the object, which is situated within the magnetic field induced between the two coils. When the magnetic field is applied, the nanoparticles generate heat which can be detected by the IR camera.

Integrating the main building blocks of the required system mentioned above comprises the system as shown in Figure 9. The system should preferably include a closed-loop feedback to allow the adjustment of the field parameters (generated by the coils) according to the temperature readings (acquired via the IR camera).

Obviously, interruption by the user (e.g., physicist) is possible, such as the tuning of magnetic field when changing its mode of operation (e.g., achieving therapy requires a substantial increase of the temperature within the treated tissue).

3. CONCLUSIONS

This system is dedicated to the detection of malignant tumors and for the treatment of those tumors based on the physical principle of heat generation for both diagnosis and therapy. The heat generation and its amplification above the body's normal temperature level are achieved by biocompatible magnetic nanoparticles which are bioconjugated to the tumor and their stimulation by a suitable external magnetic field.

This procedure is specifically targeted to the tumor since it relies on the capability of the immune system and its detectability, that is, the body knows best how to locate the malignant cells. Hence, the bioconjugation of the nanoparticles to the antigen-antibody complex is probably the most accurate method to reach the real malignancies.

The preferable configuration for the generation of the AC magnetic field in our view is the Helmholtz configuration, however the characteristics of the current generator and coils should still be evaluated.

In conclusion, this research work may serve as a novel fundamental concept for having both diagnosis and therapy in a single device, where the transfer between the two modes is merely a simple alteration of field parameters. The minimally invasive method is selective and has the potential of being very accurate, reliable, and friendly both to the operator (e.g., physician) and to the patient. It incorporates various field of research and we believe and hope that it can be developed into a bedside, cost effective, and applicable device that may assist in a better and improved detection and treatment of one of the prevalence diseases that the medical industry currently has to deal with.

4. FUTURE WORK

This research shows a fundamental design of the system which is meant to pursue thermal diagnosis and therapy in one single device which is still not bulky and can operate near the patient's bed, be accurate, reliable, and cost effective. The concept and modularly design that were described in this research work are the basis for such a system. The system comprises several main modules: heat generation (including nanoparticles and the external field generation), thermal imaging, analysis and feedback. This multidisciplinary system incorporates various scientific and technological fields. Furthermore, each module may be investigated and improved independently with no direct relation to the other modules.

Producing the required external magnetic field should be designed to generate a higher magnetic field, preferably with adjusted parameters, for example, magnitude, frequency, distance between the coils. One of the goals in our view is to increase the efficiency of this module and to enable the use of standard voltage and current one of a domestic electrical infrastructure.

The analysis module is based on the acquired raw thermal image and includes the processing for improving the data quality and derivation of desired parameters. This module may be approached by various methods implementing different mathematical models, computational algorithms, and so forth. It is desirable to try and derive additional parameters (other than tumor's depth and tumor's temperature) such as 3D geometrical boundaries of the tumor.

The current model is a basic model that relies on ideal assumptions (e.g., homogeneous tissue, steady state). Furthermore, the inverse model assumes a point source which is merely an ideal approximation for much more

complicated scenarios that involve undefined tumor boundaries, noise signals, physiological, anatomical abnormalities, and so forth.

The closed-loop feedback that allows control on the external magnetic field's parameters (e.g., magnitude and frequency) can be automatically adjusted based on the thermal imaging to maintain appropriate contrast and to achieve control on the heat expansion within the tissue in real time in order not to harm surrounding healthy tissue. This can be carried out by a LabView dedicated program.

REFERENCES

[1] F. Bretagnol and L. de Calan, "Surgery treatment of rectal cancer," *Journal de Chirurgie*, vol. 143, no. 6, pp. 366–372, 2006.

[2] Cancer Facts and Figures, 2006.

[3] L. J. Kleinsmith, D. Kerrigan, J. Kelly, and B. Hollen, "Understanding Cancer and Related Topics Understanding Cancer," National Cancer Institute, 2007.

[4] D. A. Benaron, "The future of cancer imaging," *Cancer and Metastasis Reviews*, vol. 21, no. 1, pp. 45–78, 2002.

[5] M. Ben-David, A. Inberg, I. Gannot, and N. Croitoru, "The effect of scattering on the transmission of infrared radiation through hollow waveguides," *Journal of Optoelectronics and Advanced Materials*, vol. 1, no. 3, pp. 23–30, 1999.

[6] I. Gannot, M. Ben-David, A. Inberg, and N. Croitoru, "Broadband omnidirectional IR flexible waveguides," *Journal of Optoelectronics and Advanced Materials*, vol. 3, no. 4, pp. 933–935, 2001.

[7] I. Gannot, M. Ben-David, A. Inberg, N. Croitoru, and R. W. Waynant, "Beam shape analysis of waveguide delivered infrared lasers," *Optical Engineering*, vol. 41, no. 1, pp. 244–250, 2002.

[8] N. Croitoru, A. Inberg, M. Ben-David, and I. Gannot, "Broad band and low loss mid-IR flexible hollow waveguides," *Optics Express*, vol. 12, no. 7, pp. 1341–1352, 2004.

[9] G. Fibich, A. Hammer, G. Gannot, A. Gandjbakhche, and I. Gannot, "Modeling and simulations of the pharmacokinetics of fluorophore conjugated antibodies in tumor vicinity for the optimization of fluorescence-based optical imaging," *Lasers in Surgery and Medicine*, vol. 37, no. 2, pp. 155–160, 2005.

[10] I. Gannot, A. Garashi, G. Gannot, V. Chernomordik, and A. Gandjbakhche, "In vivo quantitative three-dimensional localization of tumor labeled with exogenous specific fluorescence markers," *Applied Optics*, vol. 42, no. 16, pp. 3073–3080, 2003.

[11] V. S. Kalambur, B. Han, B. E. Hammer, T. W. Shield, and J. C. Bischof, "In vitro characterization of movement, heating and visualization of magnetic nanoparticles for biomedical applications," *Nanotechnology*, vol. 16, no. 8, pp. 1221–1233, 2005.

[12] R. Hergt, W. Andrae, C. G. d'Ambly, et al., "Physical limits of hyperthermia using magnetite fine particles," *IEEE Transactions on Magnetics*, vol. 34, no. 5, part 2, pp. 3745–3754, 1998.

[13] R. E. Rosensweig, "Heating magnetic fluid with alternating magnetic field," *Journal of Magnetism and Magnetic Materials*, vol. 252, no. 1–3, pp. 370–374, 2002.

[14] A. Jordan, P. Wust, H. Fahling, W. John, A. Hinz, and R. Felix, "Inductive heating of ferrimagnetic particles and magnetic fluids: physical evaluation of their potential for hyperthermia," *International Journal of Hyperthermia*, vol. 9, no. 1, pp. 51–68, 1993.

[15] P. C. Fannin and S. W. Charles, "Study of a ferrofluid exhibiting both Brownian and Neel relaxation," *Journal of Physics D*, vol. 22, no. 1, pp. 187–191, 1989.

[16] C. C. Berry and A. S. G. Curtis, "Functionalisation of magnetic nanoparticles for applications in biomedicine," *Journal of Physics D*, vol. 36, no. 13, pp. R198–R206, 2003.

[17] G. Glöckl, R. Hergt, M. Zeisberger, S. Dutz, S. Nagel, and W. Weitschies, "The effect of field parameters, nanoparticle properties and immobilization on the specific heating power in magnetic particle hyperthermia," *Journal of Physics: Condensed Matter*, vol. 18, no. 38, pp. S2935–S2949, 2006.

[18] R. M. Cornell and U. Schwertmann, *The Iron Oxides: Structure, Properties, Reactions, Occurrence and Uses*, John Wiley & Sons, New York, NY, USA, 1996.

[19] S. Vasseur, E. Duguet, J. Portier, et al., "Lanthanum manganese perovskite nanoparticles as possible in vivo mediators for magnetic hyperthermia," *Journal of Magnetism and Magnetic Materials*, vol. 302, no. 2, pp. 315–320, 2006.

[20] D. Bahadur, J. Giri, B. B. Nayak, et al., "Processing, properties and some novel applications of magnetic nanoparticles," *Pramana*, vol. 65, no. 4, pp. 663–679, 2005.

[21] M. Ma, Y. Wu, J. Zhou, Y. Sun, Y. Zhang, and N. Gu, "Size dependence of specific power absorption of Fe_3O_4 particles in AC magnetic field," *Journal of Magnetism and Magnetic Materials*, vol. 268, no. 1-2, pp. 33–39, 2004.

[22] H. Yin, H. P. Too, and G. M. Chow, "The effects of particle size and surface coating on the cytotoxicity of nickel ferrite," *Biomaterials*, vol. 26, no. 29, pp. 5818–5826, 2005.

[23] I. Baker, Q. Zeng, W. Li, and C. R. Sullivan, "Heat deposition in iron oxide and iron nanoparticles for localized hyperthermia," *Journal of Applied Physics*, vol. 99, no. 8, Article ID 08H106, 3 pages, 2006.

[24] P. Keblinski, D. G. Cahill, A. Bodapati, C. R. Sullivan, and T. A. Taton, "Limits of localized heating by electromagnetically excited nanoparticles," *Journal of Applied Physics*, vol. 100, no. 5, Article ID 054305, 5 pages, 2006.

[25] H. Qi and N. A. Diakides, "Thermography," in *Encyclopedia of Medical Devices and Instrumentation*, J. G. Webster, Ed., John Wiley & Sons, New York, NY, USA, 2nd edition, 2006.

[26] J. R. Oleson, T. C. Cetas, and P. M. Corry, "Hyperthermia by magnetic induction: experimental and theoretical results for coaxial coil pairs," *Radiation Research*, vol. 95, no. 1, pp. 175–186, 1983.

[27] J. P. Reilly, "Principle of nerve and heart excitation by time-variyng magnetic fields," *Annals of the New York Academy of Sciences*, vol. 649, pp. 96–117, 1992.

[28] J. R. Oleson, R. S. Heusinkveld, and M. R. Manning, "Hyperthermia by magnetic induction: II. Clinical experience with concentric electrodes," *International Journal of Radiation Oncology Biology Physics*, vol. 9, no. 4, pp. 549–556, 1983.

[29] W. J. Atkinson, I. A. Brezovich, and D. P. Chakraborty, "Usable frequencies in hyperthermia with thermal seeds," *IEEE Transactions on Biomedical Engineering*, vol. 31, no. 1, pp. 70–75, 1984.

[30] Q. A. Pankhurst, J. Connolly, S. K. Jones, and J. Dobson, "Applications of magnetic nanoparticles in biomedicine," *Journal of Physics D*, vol. 36, no. 13, pp. R167–R181, 2003.